JOC The Journal of Organic Chemistry

ARTICLE

pubs.acs.org/joc

To Bend or Not to Bend! The Dilemma of Allenes

Dhilon S. Patel and Prasad V. Bharatam*

Department of Medicinal Chemistry, National Institute of Pharmaceutical Education and Research (NIPER), Sector 67, S. A. S. Nagar (Mohali), Punjab 160 062, India

Supporting Information

ABSTRACT: Allenes, though expected to be linear, are found to be bent in many examples, especially in the case of cyclic allenes. The bending of allene is attributed to the weakening of π-bond strength across the allene. However, tetrakis-(dimethylamino)allene $\{((CH_3)N)_2C{=}C{=}C(N(CH_3)_2)\}$, which is characterized by push−push interactions, has been shown to be linear, thus leading to doubts of the current understanding of the bent allenes. In this article, we report the ab initio MO/DFT, NBO based electronic structure analysis of $R_2C{=}C{=}CR_2$ (R = H, NH_2) with a gradual increase in the number of amino substituents. The results indicate that the allenic π-bond strength and bending potential decrease, with an increase in the amino substitution. Molecular orbital analysis provides necessary clues regarding the delicate balance between orthogonality of the π orbitals and the p orbitals on the central carbon, which dictates the bending potential of the allenes. The dilemma of to bend or not to bend is a unique feature of tetraaminoallenes $(NH_2)_2C{=}C{=}C(NH_2)_2$ in comparison to isoelectronic heteroallenes $(NH_2)_2C{=}N{=}C(NH_2)_2^+$ and $(NH_2)_2C{=}B{=}C(NH_2)_2^-$.

INTRODUCTION

The chemistry of allenes[1] has fascinated experimental and theoretical scientists equally over the past several decades. Allenes are compounds with the general formula $R_2C{=}C{=}CR_2$ in which two π-bonds are orthogonal to each other with a C−C−C angle of 180°. Ab initio MO studies on the electronic structure, potential energy surface, substituent effects, rotational barrier, excited state, photodissociation, isomerization with cyclopropylidine, and Möbius character of π orbitals in allenes have been extensively reported.[2] Convenient synthetic viability and ever growing applications of allenes reported in literature triggered widespread research in this field.[1,3] The major attraction in the chemistry of allenes arises from the fact that their reactivity and selectivity can be easily tuned by modulating their electronic and steric effects by choosing appropriate substituents.[4] Therapeutic applications of products with functionalized allenic moieties, which are synthetically introduced into organic species to generate bioactive species, have been reported.[5] Comparative analyses in terms of electronic structure and effect of different substitution on physicochemical properties in the parent allenes and/or heteroallenes have been discussed in the literature.[6,7]

Bent allenes (**A**−**D**; Figure 1) are systems with nonlinear C=C=C framework, and are characterized by slightly deviated orthogonal π-bonds.[8,9] Bertrand and co-workers suggested that weakening of the π-bonds leads to bending of the C=C=C frame in allenes, which can be regulated on the basis of electron-withdrawing and -donating characteristics of the substituents.[9a,b] Structures **A** and **B** in Figure 1 represent the most severely bent acyclic and bent cyclic allenes, respectively, isolated as single crystals.[10] Cyclic allenes are bent allenes, with C=C=C angles ranging from ∼100° to 170°.[8] Though there is controversy in assigning allenic character to some of these systems,[11] the current understanding is that allenes with zwitter ionic character remain as allenes.[12] In some cases, for example in **A**, due to severe bending, the allene π system is severely disturbed, and the central carbon atom is no longer sp hybridized as in typical all-carbon allenes, but attains a unique configuration with two lone pairs of electrons and the two NHC ligands acting as donor groups.[9b] Frenking and co-workers extensively studied the electronic structure of systems **E** (core structure of **A**) and described them as divalent C(0) systems (L→C←L) with a novel bonding environment for carbon. Divalent C(0) compounds are characterized as systems (i) in which the central carbon accepts electrons from electron-donating groups, (ii) with two lone pairs on the central carbon occupying σ and π type orbitals, and (iii) with high nucleophilicity at the central carbon.[13] These compounds are found to be different from the carbenes, where the carbon atom has one σ-type lone-pair orbital and a formal oxidation state of two (divalent carbon(II)).

Frenking and co-workers reported that both allene $H_2C{=}C{=}CH_2$ and tetrakis(dimethylamino)allene $(Me_2N)_2C{=}C{=}C(NMe_2)_2$ (**F**, Figure 1) are linear;[13d,e] however, as per the suggestion by Bertrand and co-workers,[9] **F** should be highly bent (due to the push−push effect of electrons). Though reports on its existence and isolation are available,[14] experimental structural details are not available for **F**. On the other hand, computational analysis showed that tetrakis-(diethylamino)allene $(Et_2N)_2C{=}C{=}C(NEt_2)_2$ is bent with a C=C=C angle of 169°.[13c] Frenking and co-workers suggested that the C=C=C bonding environment in **F** should be considered as a donor−acceptor interaction instead of an allenic bond. This conclusion was drawn based on the comparable chemistry of **F** with divalent

Received: December 8, 2010
Published: March 17, 2011

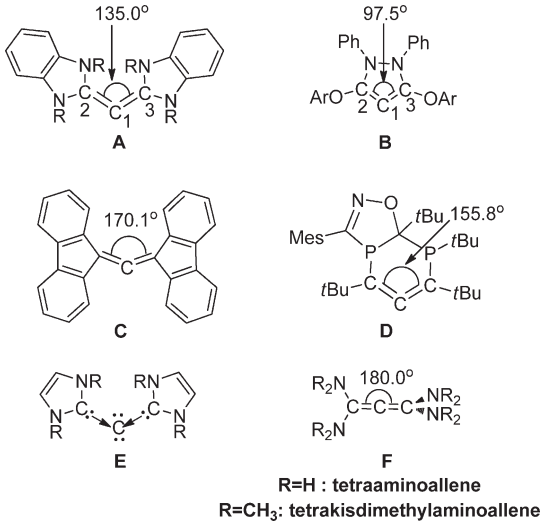

Figure 1. Bent allenes (**A**−**D**), divalent C(0) system (**E**), and linear allenes (**F**). Values shown above the structures represent the central C2−C1−C3 angles.

Scheme 1. Schematic Representation of Linear Vs Bent Geometry of Tetraaminoallene (F) and N^+ Analogue of Tetraaminoallene (G)

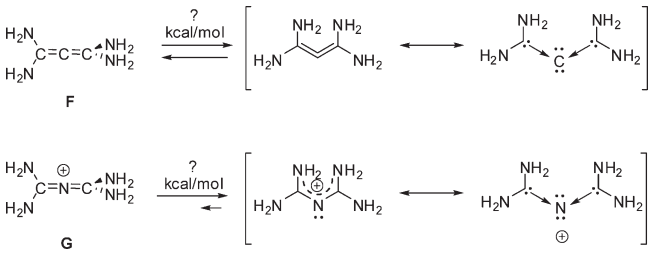

C(0) compounds in terms of their first and second proton affinities and complexation energy with BH_3.[13d] Recently, we reported geometric and electronic structure analysis of protonated biguanide $(NH_2)_2C{=}N{=}C(NH_2)_2^+$ (**G**, Scheme 1), a system isoelectronic to **F**, which is strongly bent.[15] Even though **G** is isoelectronic to allene, it was never recognized as a heteroallene due to its highly bent geometry, in fact **G** acquires characteristics similar to those of divalent C(0) compounds (**E**). It was found that many biguanide derivatives including the antidiabetic drug metformin hydrochloride,[16] $(NMe_2)(H_2N)C{=}N{=}C(NH_2)_2^+$, are shown to be electronically similar to divalent C(0) compounds.[15]

The above observations lead to some intriguing questions, examples of which follow: (i) Why **F** hesitates to bend whereas many systems with a similar central core (**A**, **C**, **E**,) are strongly bent? (ii) Is the linearity in **F** due to the two orthogonal π bonds? (iii) How the electronic structure of allenes get modified as a function of gradual increase in the electron density across C=C bonds? (iv) How the bending potential of allenes gets modulated with a gradual increase in the π electron density? (v) How the nucleophilicity at the cental carbon increases with increased π electron density? (vi) Why **F** is linear whereas isoelectronic N^+-analogue **G** is strongly bent? To address these questions, quantum chemical calculations were performed on **1**−**6**, with increasing number of NH_2 substitution in allene (**1**). The results indicate

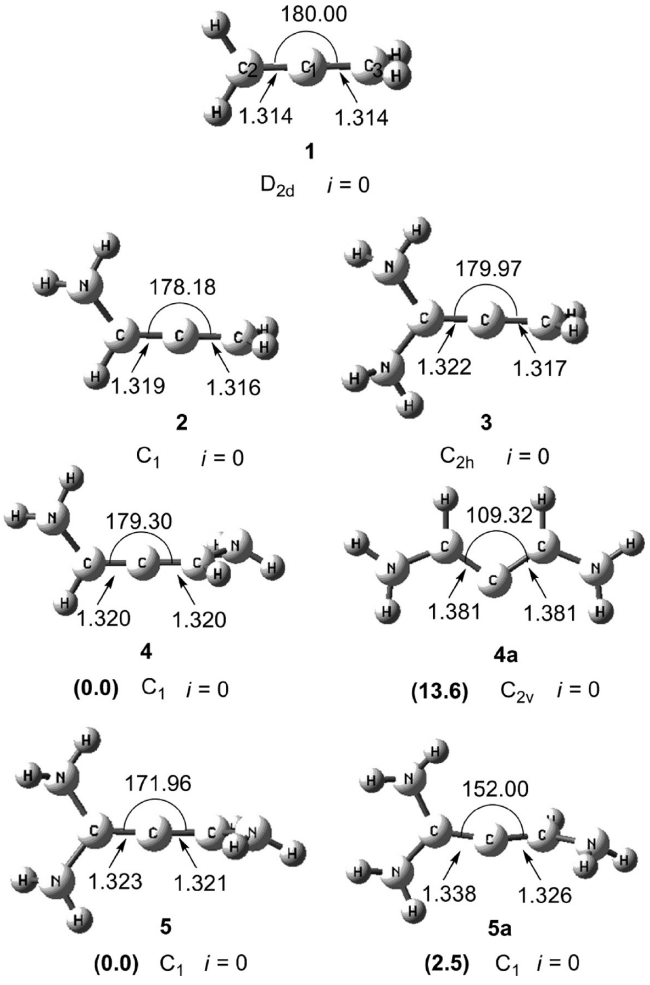

Figure 2. 3-D structural geometries of amino substituted allenes (**1**−**5**) optimized at the MP2(full)/6-31+G* level of theory. All distances are in angstrom units (Å) and angles are in degrees. *i* represents the imaginary frequency; relative energies (kcal mol^{-1}) calculated at MP2(full)/6-31+G* are given in parentheses. Nearest point groups are also given.

that **1**−**3** adopt only one structure but **4** and **5** can exist in two conformations each and **6** shows four alternative structures.

COMPUTATIONAL DETAILS

Ab initio MO[17] and density functional theory (DFT)[18] calculations were carried out using the GAUSSIAN03 package.[19a] Complete optimizations without any geometric as well as symmetry constraints were performed on the aminoallenes $R_2C{=}C{=}CR_2$ (R = H, NH_2) (**1**−**6**, Figures 2 and 3) using B3LYP[20] and MP2(full)[21] methods with the 6-31+G* basis set. Calculations were performed on the methyl derivatives (**7** and **8**, Figure 3) of **6** also. Frequencies were computed analytically for all optimized species at all levels to characterize each stationary point as a minimum or a transition state, and also to estimate the zero-point vibrational energies (ZPE). The calculated ZPE values (at 298.15 K) have been scaled by a factor of 0.9806 and 0.9661 for B3LYP and MP2(full) levels, respectively.[22] The final energies were obtained by using the high accuracy G2MP2 calculations.[23] The discussion of relative energies is based on the G2MP2 free energies (unless otherwise specified) and geometrical parameters observed in the MP2(full)/6-31+G* optimized structures. NBO analysis[24] was performed on **1**−**6** with use of the MP2(full)/6-31G* level of theory. Single and double proton affinities and complexation energies with BH_3 and AuCl were

dx.doi.org/10.1021/jo102432a |J. Org. Chem. 2011, 76, 2558–2567

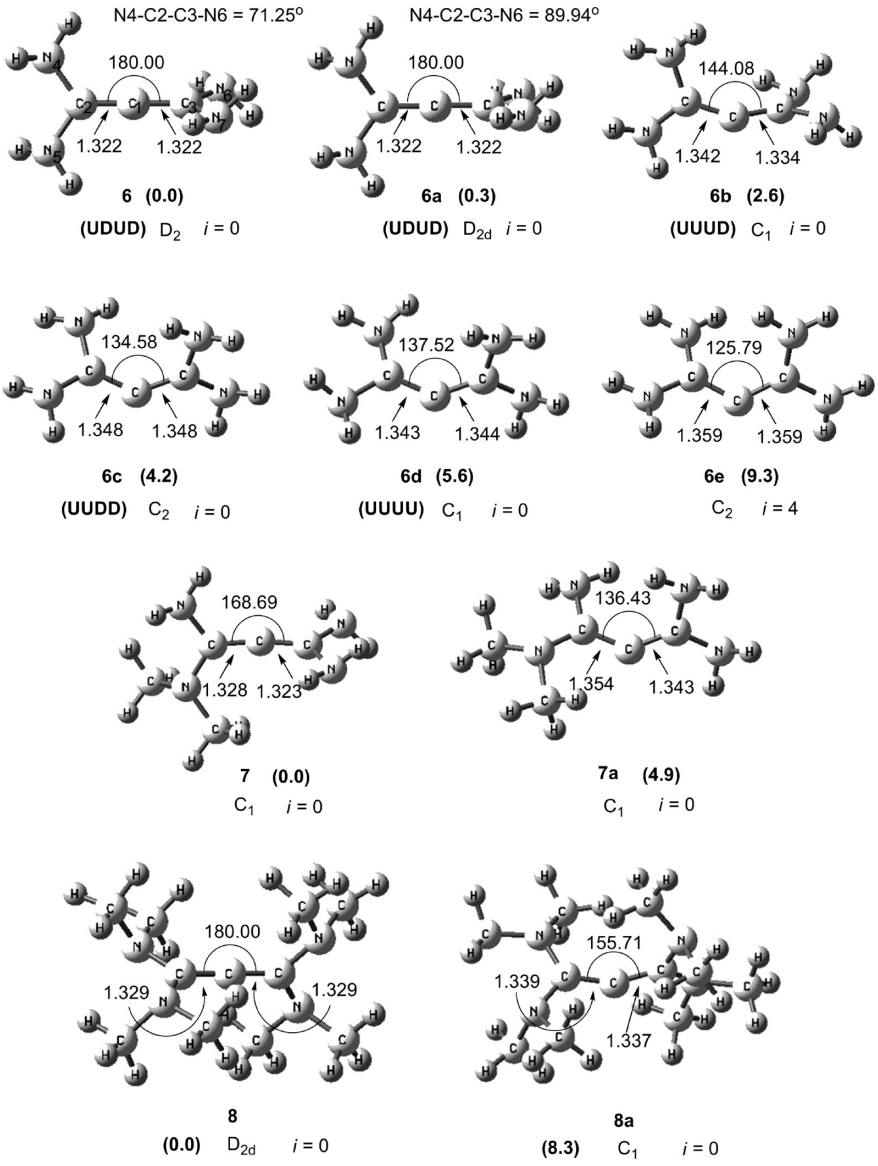

Figure 3. 3-D structural geometries of amino substituted allenes (**6** and its derivatives) optimized at the MP2(full)/6-31+G* level of theory. All distances are in angstrom (Å) units and angles are in degrees. *i* represents the imaginary frequency; relative energies (kcal mol^{-1}) calculated at MP2(full)/6-31+G* are given in parentheses. Nearest point groups are also given.

also estimated for each member of this series. Complexes of **1**−**8** with AuCl were optimized with the mixed basis set 6-31+G* plus def2-TZVPP.[25] Figure 2 shows the 3D structures of **1**−**5** and Figure 3 shows the 3D structures of **6** and its methyl derivatives. The relative energies, rotational barriers, and inversion barriers in **1**−**6** are listed in Table 1. Calculations were also performed on $R_2C{=}E{=}CR_2$ ($E = B^-, N^+$) analogues of **1** and **6**.

RESULTS AND DISCUSSION

Structural Analysis of Amino-Substituted Allenes. Complete optimization showed that allene $H_2C{=}C{=}CH_2$ (**1**) is linear (as expected) with a C2−C1−C3 angle of 180°. This angle gets slightly reduced upon NH_2 substitution in **2** (178.2°), **3** (180°), and **4** (179.3°) at the MP2(full)/6-31+G* level. However, in **5** the C2−C1−C3 angle is about 172°, indicating that the bent allene character is present in triaminoallene. Tetraaminoallene **6** again shows a linear structure. Structures **4a** and **5a** (Figure 2) are the structural isomers for **4** and **5**, respectively; **6a**−**d** are structural isomers of **6** (Figure 3).

Triaminoallene shows two minima **5** and **5a** with C2−C1−C3 angles 172° and 152°, respectively. Both of them possess two (almost) orthogonal π-bonds. The major difference between these two isomers arises due to N-inversion at the $C(NH_2)_2$ center UU or UD (U = up, D = down with reference to pyramidalization of NH_2 groups). The ΔE between the two structures is about 1.2 kcal mol^{-1}, **5** being more stable. **4a** cannot be considered as an allene because the π frame in this species does not show orthogonal character.

Several minima are found on the ground state potential energy (PE) surface of tetraaminoallene **6** (i.e., **6** and **6a**−**d**). **6** and **6a** are characterized by UDUD arrangements of NH_2 groups with linear arrangement. **6** is the most stable structure on its PE surface, which shows a N−C2−C3−N torsional angle of 71.3° while **6a** with a N−C2−C3−N torsional angle of ∼90° is only

dx.doi.org/10.1021/jo102432a |J. Org. Chem. 2011, 76, 2558–2567

Table 1. Relative Energies and Rotational Barriers (in kcal mol^{-1}) in 1−8, Estimated Using Quantum Chemical Methods (6-31+G* basis set employed)

structures	B3LYP[d]	MP2(full)[d]	G2MP2[a]
4−**4a**	13.3	13.6	16.3
5−**5a**	2.3	2.5	1.2
6−**6a**	0.1	0.3	0.1
6−**6b**	2.4	2.6	1.4
6−**6c**	4.5	4.2	2.6
6−**6d**	5.4	5.6	—[b]
6−**6e**	7.9	9.3	6.7
7−**7a**	4.4	4.9	3.6
8−**8a**	2.9	8.3	—[c]
1-RT	71.9 (43.7)	72.2 (53.9)	71.8
2-RT	33.0 (37.8)	33.6 (50.0)	35.9
3-RT	23.7 (37.8)	24.7 (50.5)	25.2
4-RT	24.2	25.5	26.3
5-RT	12.7	14.0	15.7
6-RT	14.2	14.7	16.4
7-RT	15.8	17.1	18.8
8-RT	29.6	32.1	—[c]

[a] G2MP2 free energy data at 298.15 K. [b] Geometry was not properly converged at the G2MP2 level. [c] Due to limited resource of computational power, optimization at G2MP2 was not carried out. Values in parentheses show the rotational barriers for open shell transition states. [d] Values in parentheses show the rotational barriers for open shell transition states.

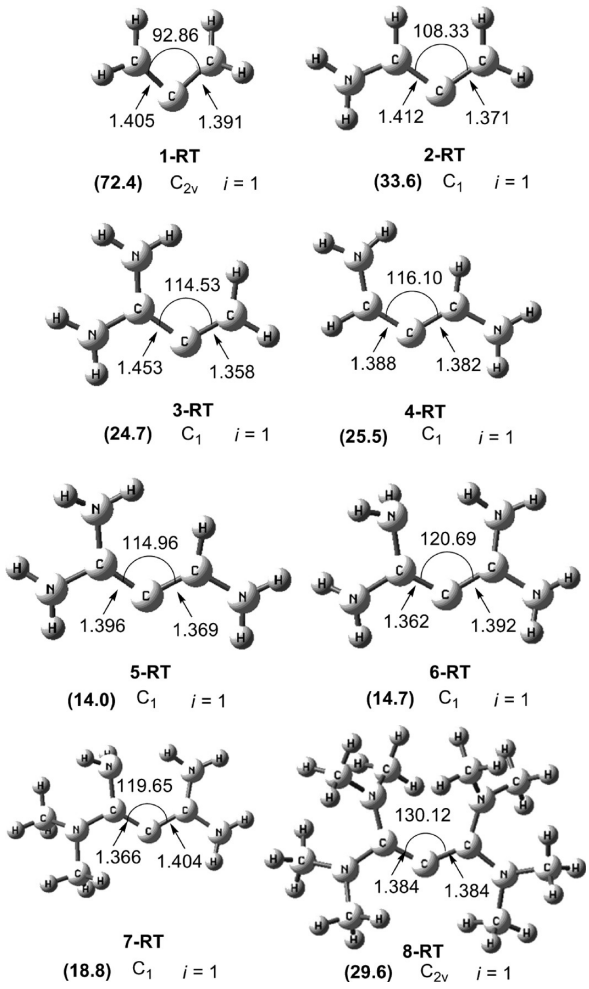

Figure 4. 3-D structural geometries of rotational transition states in **1**−**8** optimized at the MP2(full)/6-31+G* level of theory. All distances are in angstrom units (Å) and angles are in degrees. i represents the imaginary frequency; relative energies (kcal mol^{-1}) calculated at the MP2(full)/6-31+G* are given in parentheses. Nearest point groups are also given.

about 0.1 kcal mol^{-1} higher in energy. Greater stability of **6** over **6a** is presumably due to stabilization arising from Möbius type electron delocalization.[2l] **6b** adopts the UUUD arrangement of the NH_2 groups, with the C2−C1−C3 angle of 144.1° and the N−C2−C3−N torsional angle of 81°, and is about 1.4 kcal mol^{-1} higher in energy. **6c** adopts the UUDD arrangement of NH_2 groups (C2−C1−C3 angle 134.6°, N−C2−C3−N torsional angle 60.2°) and is 2.6 kcal mol^{-1} higher in energy. **6d** with the UUUU arrangement of NH_2 groups (C2−C1−C3 angle 137.5°, N−C2−C3−N torsional angle 70.4°) could be located only at the MP2(full) level and is even less stable. The existence of several alternative structures for **6** within 3−5 kcal mol^{-1}, the lack of orthogonal planes in many of them, and strongly bent arrangement in these alternative structures clearly indicate the very weak C═C═C π bonds in **6**. This weakness leads to a shallow bending potential and the apparent linearity in **6**. When the NH_2 groups are forced to adopt local planarity in structure **6e** (to mimic the planar N-heterocyclic carbene (NHC) type structure as in **E** (Figure 1); with four negative frequencies), the C2−C1−C3 angle became very small at 125.8° and the structure is 6.7 kcal mol^{-1} higher in energy.

Substituents on **6** break the symmetry and expose the weak π bonds, and thus bend the allenes. In the *N*,*N*-dimethyl derivative of **6** (i.e., **7**), a carbon analogue of blockbuster drug metformin hydrochloride, the NR_2 groups adopt the UDUD arrangement, similar to **6**, and become bent with a C2−C1−C3 angle of 168.7°. This suggests that breaking of the molecular symmetry from **6** to **7** favors bending of the allene. The alternative UUDD (NR_2) structure **7a** shows a strongly bent arrangement (C2−C1−C3 angle of 136.4°). The octamethyl derivative **8** (same as **F**) preferred to be linear (180°)[13d] while its structural isomer **8a** (with UUDD NR_2 orientation) has a bent structure with a C2−C1−C3 angle of 155.7° and it is only 8.3 kcal mol^{-1} less stable than the corresponding linear structure (**8**) at the MP2(full)/6-31+G* level of theory. Tonner and Frenking reported the structural features of octaethyltetraaminoallene which showed a bent C2−C1−C3 angle of 169.5°, and attributed this phenomenon to the shallow bending potential.[13d] To further verify this, the heptamethyl derivative of **6** was also studied, which showed a C2−C1−C3 angle of 169.7°.

C═C Rotational Process in Amino Substituted Allenes. Seeger et al. studied the C═C rotational process in allene through a C_{2v} bent planar structure. The barrier through the $^1A_1$ state was shown to require 76.4 kcal mol^{-1}.[2a] But in comparison to the experimental value,[2b,c] it was corrected and the rotational transition state has been reported to go through a $^1A_2$ state with a barrier of 50.1 kcal mol^{-1}.[2a] Jarowaski et al. reported that substitution drastically reduces C═C rotational barriers in alkenes;[26] in allenes also C═C rotational barriers are expected to reduce significantly. Especially in allenes with electron-donating amino groups, the barrier is expected to be quite small. To verify

dx.doi.org/10.1021/jo102432a |*J. Org. Chem.* 2011, 76, 2558–2567

Table 2. Partial Atomic Charge Analysis (given in electron) on Central Core Atoms of $R_2C{=}C{=}CR_2$ Obtained by Using the NBO Method in 1−8

	charge on central core atoms of $R_2C{=}C{=}CR_2$ (R = NH_2)		
compd	C2	C1	C3
1	−0.519	0.073	−0.519
2	−0.050	−0.059	−0.475
3	0.352	−0.136	−0.455
4	−0.003	−0.211	−0.003
5	0.400	−0.300	0.020
6	0.415	−0.378	0.415
7	0.443	−0.358	0.421
8	0.422	−0.271	0.422
5a	0.451	−0.372	−0.023
6b	0.431	−0.478	0.476
6c	0.476	−0.548	0.476
6d	0.460	−0.517	0.478

this, the C=C rotational process in systems **1** to **6** was evaluated by using open shell as well as close shell wave functions. The results indicate that PE surface of **1**−**3** show the presence of open shell singlet diradical transition states (TS); however, only in case of **1** is bending of the C=C=C preferred through open shell singlet diradical TS (barrier of ∼54 kcal mol^{-1} at the UMP2-(full)/6-31+G* level) over close shell TS (**1-RT**, barrier of ∼72 kcal mol^{-1} at the MP2(full)/6-31+G* level). These rotational barriers for **1** are comparable to the previously reported studies on allene rotations.[2a,27] For **2** and **3** open shell singlet diradical TS (50.0 and 50.5 kcal mol^{-1} respectively at the UMP2(full)/6-31+G* level) are found to be higher than the close shell singlet TS (33.6 (**2-RT**) and 24.7 (**3-RT**) kcal mol^{-1} respectively at the MP2-(full)/6-31+G* level). These data suggest that on monoamino (**2**) and diamino (**3**) substituted allene, there is a crossover from open shell TS to close shell TS. On further increasing the number of amino substitutions from **4**−**6**, no open-shell TS exists. For this reason further discussion on C=C rotational barrier results is based on close shell TS.

The barrier for the C=C rotation in **4** is 26.3 kcal mol^{-1} at the G2MP2 level (Table 1), which is quite comparable to that of **3** but much smaller than that in **1** and **2**. The C=C rotational barriers in **5** and **6** are 15.7 and 16.4 kcal mol^{-1}, respectively, much smaller than that from **1**−**4**, suggesting the weakening of the π-bond due to increased electron delocalization from NH_2 groups. The rotational transition state **6-RT** is characterized by an intramolecular hydrogen bond with a bond length of 2.08 Å. The small values of C=C rotational barrier in **5** and **6** clearly indicate that these species are characterized by a high degree of flexibility and they should be in the dynamical state. The triaminoallene shows a C1-inversion barrier of about 9 kcal mol^{-1}, adding further to its flexibility. Similar to **6-RT**, the rotational transition state for **7** is also characterized by an intramolecular hydrogen bond with a bond length of 2.08 Å. The C=C rotational barrier in **7** is 18.8 kcal mol^{-1}, similar to **6** and much smaller than that in **1**−**4**. The C=C rotational barrier in **8** at the MP2(full) level is 32.1 kcal mol^{-1}, which is much larger than that of **6** and **7**; this can be attributed to the presence of steric clashes in **8-RT**. The gradual decrease in the C=C rotational barriers in **1**−**6**

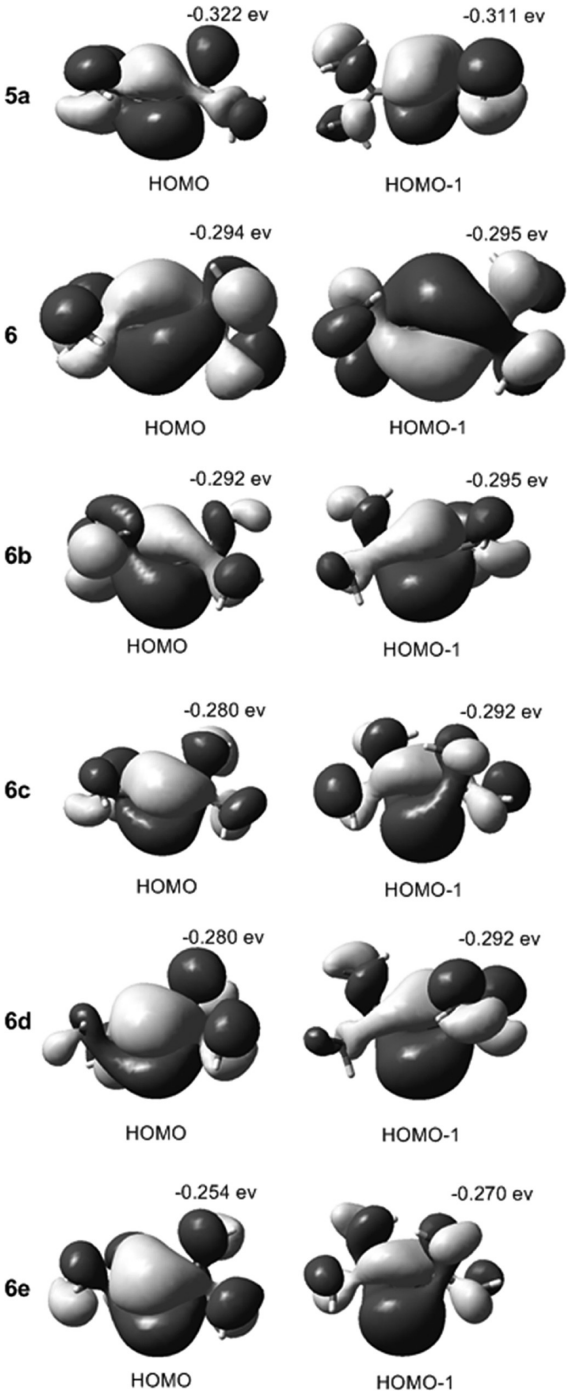

Figure 5. Shape of the π and σ type lone pair MOs on the central carbon atom of **5**, **6**, and **6b**−**e** generated from the MP2(full)/6-31+G* optimized geometries.

support the suggestion by Bertrand that the π strength in allene gradually decreases with an increase in the electron donation to these π bonds. The extra electron density from the lone pairs of the substituent amino groups being "pushed" reaches the π^* orbital of allene and hence weakens the π bonds. Even in **6** and **8**, where linearity is preferred, the C=C π strength is weak (Figure 4).

Natural Bond Orbital (NBO) Analysis. NBO[24] charge analysis showed that there is a gradual increase in the negative charge

dx.doi.org/10.1021/jo102432a |J. Org. Chem. 2011, 76, 2558–2567

Scheme 2. The π Molecular Orbital Rehybridization in 6 in Relation to the Molecular Orbitals in 1

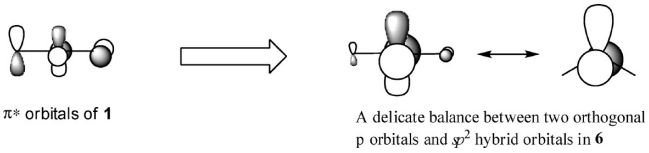

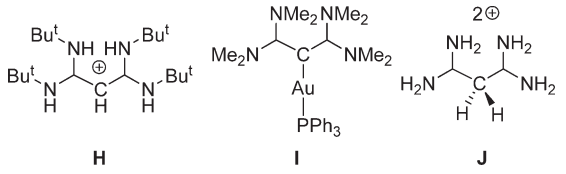

Figure 6. Schematic representation of crystallographically known protonated and metal complexes of various tetraaminoallene derivatives.

localization at the central carbon on going from **1** to **6** (Table 2). Such polarization of allenic π bonds toward the central carbon atom in cyclic bent allenes was also noted by Bertrand and coworkers.[10,12] In **1**, the central C1 carried a very small positive charge of 0.073 at the MP2(full)/6-31+G* level. Upon introducing one NH_2 group in **1** (**2**), C1 becomes negatively charged (−0.059). The negative charge gradually increased in **3**−**6** in the order −0.136, −0.211, −0.300, −0.378. The atomic charge on C1 in the strongly bent **5a** is −0.372. The bent structures of **6** are characterized by much greater charge at C1: −0.478 (**6b**), −0.548 (**6c**), and −0.517 (**6d**) in comparison to −0.378 in **6**. Detailed NBO analysis (Table S1, Supporting Information),[19b] showed an increase in the $n_N \rightarrow \pi^*_{C=C}$ delocalization in **2**−**6**. This electron delocalization decreases π strength and increases charge localization at C1. The $n_N \rightarrow \pi^*_{C=C}$ delocalization in **6** is ∼117 kcal mol^{-1}, which increases further in **6b**, **6c**, and **6d** to ∼134, ∼144, and ∼148 kcal mol^{-1} respectively. Analysis of the NBO results in greater detail also revealed that as the $n_N \rightarrow \pi^*_{C=C}$ increases, the coefficient of the p orbital at the central carbon increases and the coefficient of the p orbitals of the terminal carbon decrease. This also leads to uneven overlap of p orbitals and leads to decrease in the π overlap and hence the π strength. This C=C=C π weakening can indeed facilitate divalent C(0) character at the cental carbon of **6**; however, its linear structure prevents such a possibility. In the bent alternatives **6b**−**d** two lone pairs on C1 can be noticed as per the MO analysis (Figure 5).

Molecular Orbital (MO) Analysis. Molecular orbital (MO) analysis (Figure 5) shows that the two π bonds in **6** are characterized by large p lobes on the central carbon and very small p lobes on the terminal carbons, thus weakening the π bonds. In **1**, the orthogonality is due to the two π orbitals, which enforces sp character at the central carbon. In **6**, because of the decrease in the π strength and an increase in the p orbital contribution on the central carbon, the forces between the two orthogonal π orbitals of the allenes decrease and reduce the compulsion to maintain orthogonality. The natural tendency of carbon is to show great hybridization between s and the p orbitals and prefers the $sp < sp^2 < sp^3$ hybridization. This natural tendency takes over when opportunity for rehybidization is available as in **6b**−**d**. In **6**, however, the two p orbitals on the central carbon are perfectly equivalent and hence continue to exert equal forces and make the molecule linear. Scheme 2 gives a pictorial representation of

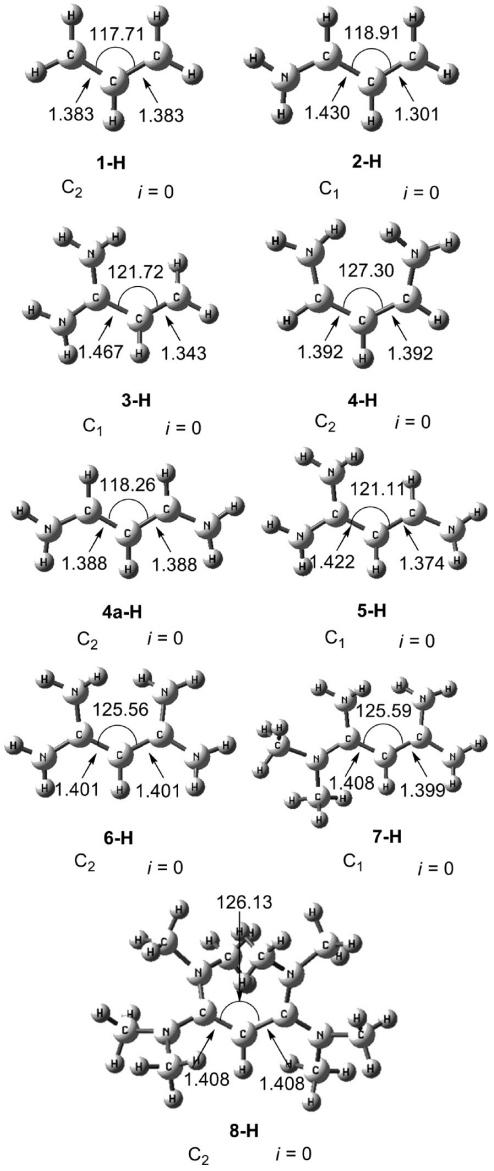

Figure 7. 3-D structural geometries of protonated species of **1**−**8** optimized at the MP2(full)/6-31+G* level of theory. All distances are in angstrom (Å) units and angles are in degrees. $i = 0$ represents the minimum. Structures of diprotonated species are given in the Supporting Information.[19b] Nearest point groups are also given.

the changes on the π^* orbitals of allene as a function of tetraamino substitution. A delicate balance between the weak π bonds and sp^2 rehybridization exists in allenes substituted with electron-donation groups. Upon reducing the symmetry across the central carbon, this balance tilts toward sp^2 structures. This delicate balance dictates the angle across the C−C−C central core of substituted allenes. Thus, a unique opportunity is available to stabilize systems with varying angles across the central carbon in allenes. Exploring this delicate balance shall help in generating systems with a spectrum of angle between 120° to 180° around carbon.

In the bent alternatives **6b**, **6c**, and **6d**, two lone pairs on C1 can be observed (as in divalent C(0) systems) according to MO analysis. This becomes clearly evident in **6e**, in which the charge on the central carbon C1 was found to be −0.652, much larger than the charge on C1 in **6** (−0.378). Such a restricted structure

dx.doi.org/10.1021/jo102432a |J. Org. Chem. 2011, 76, 2558–2567

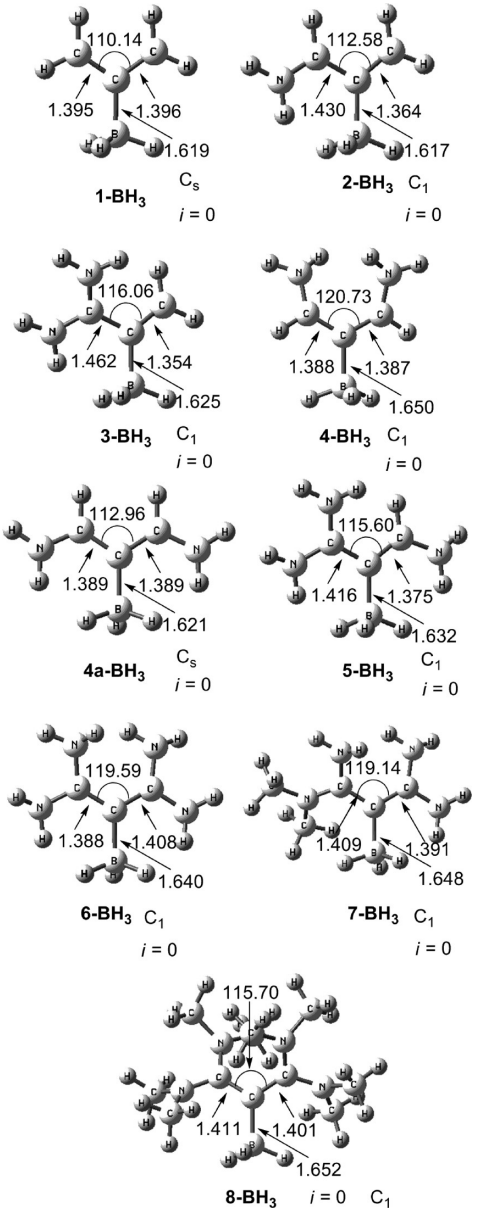

Figure 8. 3-D structural geometries of BH_3 complexes of **1**−**8** optimized at the MP2(full)/6-31+G* level of theory. All distances are in angstrom (Å) units and angles are in degrees. $i = 0$ represents the minimum. Structures of species with coordination with two BH_3 units are given in the Supporting Information.[19b] Nearest point groups are also given.

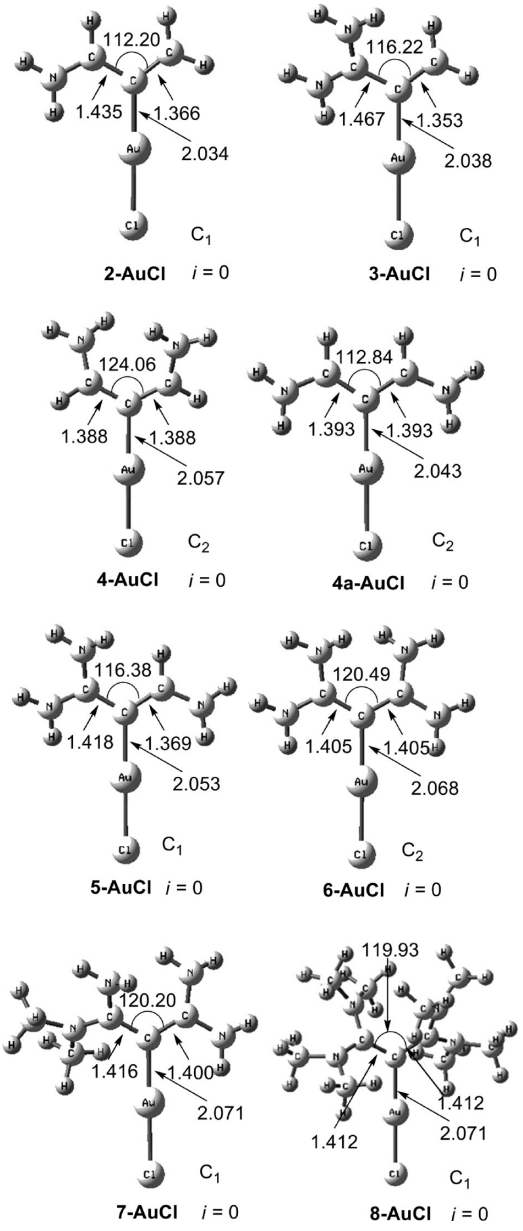

Figure 9. 3-D structural geometries of AuCl complexes of **1**−**8** optimized at the MP2(full)/6-31+G* level of theory. All distances are in angstrom (Å) units and angles are in degrees. $i = 0$ represents the minimum. Structures of species with coordination with two AuCl units are given in the Supporting Information.[19b] Nearest point groups are also given.

is characterized by two lone pairs at the central carbon occupying π-based HOMO and σ-based HOMO-1 as per MO analysis, tending toward divalent C(0) like character.[13c,d] It is worth noting that in divalent C(0) compounds based on NHCs (**A** and **G**), the planarity at nitrogen is forced due to the rings in NHC (very similar to **6e**).

Proton Affinities and Complexation Energies. The bent allenes tend to behave like carbenes/divalent C(0) systems and thus become highly nucleophilic. The nucleophilicity of **1**−**8** is expected to increase with an increase in the amino groups. The following experimental facts support this expectation. Tetraaminoallene and dialkoxydiaminoallene are reported to be highly nucleophilic at the central carbon (C1).[14] Synthesis and chemistry of protonated tetraaminoallenes are reported, and the crystal structure of the 1,1,3,3-tetrakis(tertbutylamino)allyl cation (**H**, Figure 6) is reported. Similarly, a complex of tetraaminoallene with $AuPPh_3$ (**I**, crystal structure available) is reported, which also supports the higher nucleophilicity of the tetraaminoallenes.[13k,l] A second protonation is also expected in **6**−**8**. The crystal structure evidence for diprotonated melanodiamidine (**J**) provided proof for the high nucleophilicity as well as divalent C(0) character for tetraaminoallene.[28]

Proton affinities and complexation energies with BH_3 and AuCl provide clues regarding the extent of divalent C(0) character of bent allenes. Carbenes show strong first proton affinity but low second proton affinity whereas divalent C(0) compounds show much stronger first and second proton affinities.[13c,e] The

Table 3. Proton Affinities and Complexation Energies in kcal mol^{-1} (with BH_3 and AuCl) of 1−8 Calculated at B3LYP,MP2(full) Using the 6-31+G* Basis Set and the G2MP2 Level of Theory[a]

	proton affinity						BH_3 complexation						AuCl complexation	
	first			second			first			second			first	second
compd	B3LYP	MP2	G2MP2	B3LYP	MP2	G2MP2	B3LYP	MP2	G2MP2	B3LYP	MP2	G2MP2	B3LYP	B3LYP
1	178.41	174.74	184.11	−4.82	−9.90	−2.03	−23.06	−22.57						
2	229.32	227.90	237.45	32.12	28.72	38.43	20.86	25.24	15.29				40.31	
3	248.55	247.62	257.46	45.66	40.17	49.43	33.65	37.72	28.00	5.59	10.58	6.23	52.24	32.99
4	245.88	242.79	252.16	86.49	88.47	100.11	20.51	23.48	12.55	12.63	17.94	16.53	43.38	40.96
5	265.95	262.37	272.06	98.93	100.27	111.86	44.14	47.13	37.36	5.20	12.74	5.19	63.10	34.09
6	272.89	268.95	278.65	118.98	119.41	131.69	44.91	48.51	39.34	9.89	17.80	9.45	63.70	37.39
7	275.55	270.89	281.48	129.72	134.50	142.01	39.34	43.73	33.74	15.60	24.38	15.41	59.23	42.24
8	273.56	269.81		142.65	140.92		25.62	33.90		−1.41	10.34		47.99	36.96

[a] For the AuCl complex we have used the 6-31+G* basis set for C, H, N while AuCl was treated with the def2-TZVPP basis set.

geometric features of **1**−**8** upon protonation, upon BH_3 complexation, and upon AuCl complexation are given in Figures 7, 8, and 9, respectively. The MP2 optimized structural features of **8-H** are quite comparable to that of the crystal structure data on 1,1,3,3-tetrakis(tertbutylamino)allyl cation (**H**, Figure 6) (especially the C2−C1−C3 angle 126.13° in **8-H** and 127.1° in the crystal structure).[14d] Similarly, the geometric features of **6-2H** (Figure S1, Supporting Information)[19b] are quite comparable to that of malanodiamide[28] (**J**) (the C2−C1−C3 angle is 116.2° for the crystal structure and 114.3° for the MP2 estimate). The calculated structural features of the AuCl complex of **C-8** are comparable to the crystal structure of th $AuPPh_3$ complex of **C-8** (**I**) (the C2−C1−C3 angle is 119.9° in **C-8-AuCl** and 118.5° in the crystal structure of **I**). Thus, the estimation of proton affinities and BH_3 and AuCl complexation energies of **1**−**8** can give clues to the hidden divalent C(0) character in these systems.[13k,l]

Table 3 shows the estimated first and second proton affinities and complexation energies with one and two BH_3 units of **1**−**8** at three different quantum mechanical methods. Also listed in Table 3 are the B3LYP/(6-31+G* plus def2-TZVPP) estimated complexation energies of **1**−**8** with one and two AuCl units. The first proton affinities increase from 174.7 to 269.8 kcal mol^{-1} in **1**−**8**. The first BH_3 complexation energies range between 25 and 48 kcal mol^{-1} in **1**−**8**. In **7** and **8** the BH_3 complexation energies are relatively smaller than that of **6**, because of steric factors. Similarly, the complexation energies of **1**−**6** with AuCl increase in the order 40−63 kcal mol^{-1}, with **7** and **8** showing marginally smaller values in relation to **6**. This may also be attributed to the decreased charge on C1 in **7** and **8** in comparison to **6**. These data clearly confirm that there is a gradual increase in the nucleophilicity of **1**−**8** with an increase in the electron-donating substituents in allenes. The second proton affinity, the complexation energies due to a second BH_3 as well as a second AuCl also show a gradual increase (Table 3). Especially **6**−**8** do indeed possess characteristics of divalent C(0) systems as indicated by strong second proton affinity values and small but significant complexation energies due to a second BH_3 and a second AuCl.

N^+ and B^- Analogues of 6. To further verify the bending dilemma of the allenes, a similar computational analysis was performed on isoelectronic N^+ and B^- analogues, $R_2C{=}N{=}CR_2{}^+$ and $R_2C{=}B{=}CR_2{}^-$. These systems are examples of heteroallenes with th general formula $R_2C{=}E{=}CR_2$. Quantum chemical analysis showed that $H_2C{=}N{=}CH_2{}^+$ (**N-1**) (Figure 10) and $H_2C{=}B{=}CH_2{}^-$ (**B-1**) are linear species with the two π-bonds orthogonal to each other, quite similar to **1**. The C═N rotational barrier in **N-1** is 41.2 kcal mol^{-1} at th G2MP2 level, which is much smaller than that in **1** (71.8 kcal mol^{-1}). The C═B rotational barrier in **B-1** is 75.7 kcal mol^{-1} at the G2MP2 level, which is slightly higher than the C═C rotational barrier in **1**. These differences may be originating from the differences in the $\pi-\pi$ overlap across the E═C bonds. It is interesting to note that the E═C bond rotational barriers in **B-1**, **1**, and **N-1** are on the order of 75.7, 71.8, and 41.3 kcal mol^{-1}, respectively, clearly indicating that the E═C π strength decreases across a period. It also suggests that the differences among **B-1**, **1**, and **N-1** are significant though these systems are isoelectronic.

The tetraamino-substituted system **B-6** is linear (180°) whereas **N-6** is completely bent (122.8°).[16] The C═E rotational barriers in **B-6** and **N-6** are 36.3 and 2.7 kcal mol^{-1}, repectively, at the G2MP2 level. These values are completely different from the C═C rotational barrier in **6** (16.4 kcal mol^{-1}). Tetraamino substitution decreases the π strength in **1** (rotational barrier reduced from 71.8 (53.9 open shell RT) to 16.4 kcal mol^{-1}), **B-1** (rotational barrier reduced from 75.7 to 36.3 kcal mol^{-1}), and **N-1** (rotational barrier reduced from 41.2 to 2.7 kcal mol^{-1}). A bent alternative structure of **B-6** shows a C−B−C angle of 168° and is ∼7 kcal mol^{-1} higher in energy, indicating that bending is not a favorable process in **B-6**. The bending probability is very low for **B-6**, very high for **6**, but compulsory for **N-6**. The influence of tetraamino substitution is dramatic in **N-1** but negligible in **B-1**; on the other hand, the influence of tetraamino substitution on **1** is intermediate. Substitution in **B-1** does not bend the system, substitution in **N-1** completely bends the system, whereas substitution in **1** leads to an apparent dilemma "to bend or not to bend in allenes". The above analysis indicates that although the bending potential becomes shallower along the row (B > C > N) - the dilemma "to bend or not to bend" is a unique feature of tetraaminoallenes $(NH_2)_2C{=}C{=}C(NH_2)_2$, but in isoelectronic **B-6** and **N-6** no such dilemma exists.

From the above analysis on **1**−**6**, it is clear that the C2−C1−C3 angle tends to bend with an increase in the NH_2 substitution. The triaminoallene **5** acquires a bent allene like character. The tetraminoallene structural isomers **6b**, **6c**, and **6d** with strongly bent arrangements (144.1°, 134.6°, and 137.5°) are possible because of the shallow bending potential. The C═C π strength gradually decreases with an increase in the NH_2 substitution (i.e.,

dx.doi.org/10.1021/jo102432a |J. Org. Chem. 2011, 76, 2558–2567

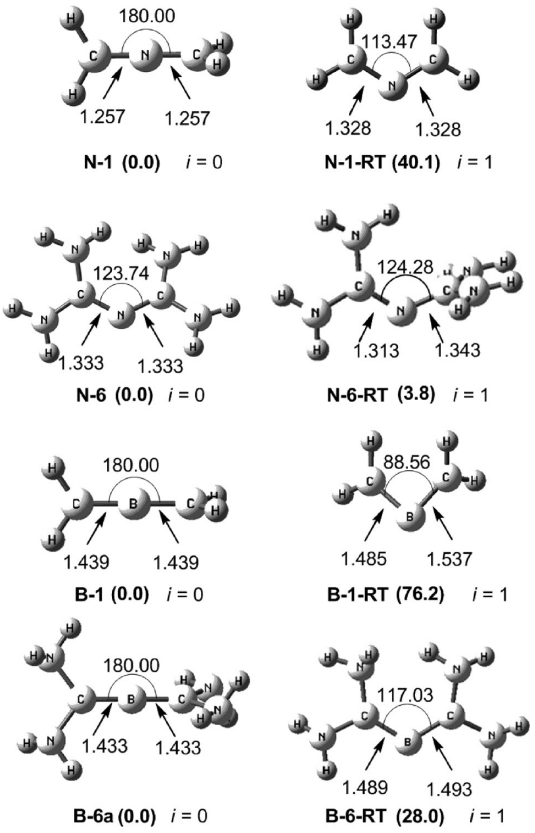

Figure 10. 3-D structural geometries of N^+ and B^- analogues of **1** and **6** with the corresponding rotational transition states optimized at the MP2(full)/6-31+G* level of theory. All distances are in angstrom units (Å) and angles are in degrees. *i* represents the imaginary frequency; relative energies (kcal mol^{-1}) calculated at the MP2(full)/6-31+G* are given in parentheses.

Scheme 3. Gradual Transformation of Allenes (K) to the Divalent C(0) System (L) with an Increase in Donor Substituents

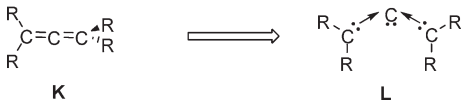

with an increase in the electron pumping to the π^* orbital), thus, weakening of π bond in allene does indeed induce bent allene character to allenes. A delicate balance between the orthogonal π orbitals vs the orthogonal p orbitals on the central carbon determines the bending potential of substituted allenes. Though the decrease in π strength does not immediately reflect in bending the allenes, it indeed facilitates the dynamical state of allenes. The charge localization at C1 increases with an increase in the NH_2 substitution. This gives a much clearer signal, i.e. decrease in π strength across C═C in allenes parallels with an increase in the charge localization at the central carbon. The nucleophilicity of **1**−**6** increase in the same order, indicating that the NH_2 substitution induces divalent C(0) character. Allenes tend to acquire divalent C(0) character as in **6b**−**d** with increasing NH_2 substitution. On the other hand, they remain linear with electron-demanding substituents.[29] Thus, the electronic structure of allenes with highly π donating substituents tends to move toward **L** from **K** (Scheme 3) with a gradual increase of such substituents. This can be exploited to identify open chain allenes with a spectrum of C−C−C angles between 180° and 120°.

CONCLUSIONS

Electronic structure of a series of amino-substituted allenes $R_2C{=}C{=}CR_2$ (R = H, NH_2) was explored to elucidate the bent vs linear character of these systems. Three different electronic structural environments are competing in these systems: (case I) with orthogonal π bonds as in allenes, (case II) with π conjugated systems with one lone pair on the central carbon such as in carbene, and (case III) a bent allene character with two lone pairs on the central carbon as in divalent C(0) systems. Results based on different analyses generated a clear picture to confirm the structural preference of amino-substituted allenes. The detailed electronic structure analysis proved that the C═C π bond strength decreases with an increase in the NH_2 substitution of allenes. Molecular symmetry as well as NH_2 group orientation also contribute significantly in determining the bending of allenes. NBO analysis also suggested that charge accumulation at the central C increases with an increases in the number of NH_2 groups. The decrease in C═C rotational barriers of allene upon amino substitution also suggest gradual conversion from allenic bond (**1**) to donor−acceptor bond (**6**). In **6**, the orthogonality is due to the two p orbitals on the central carbon but not due to the two π orbitals, hence the orthogonality is very weak and tends to bend when symmetry is broken. Furthermore, the estimated proton affinities, the nucleophilicity parameters, and their gradual change as a function of increasing amino substitution support the observed changes in allene vs divalent C(0) character of the species. In the case of amino-substituted heteroallenes $R_2C{=}E{=}CR_2$ (R = H, NH_2), isoelectronic B^- analogues are clearly linear, whereas N^+ analogues are clearly bent. The detailed analysis suggests that it is only a distinct character of all carbon allenes which show the dilemma of "to bend or not to bend" upon substitution. This unique position of all carbon allenes is responsible for extended interest in this class of compounds.

ASSOCIATED CONTENT

Supporting Information. Detailed NBO analysis of the selected species (Table S1), absolute energies of all the geometries under consideration(Tables S2 and S3), the coordinates and absolute energies of the optimized geometries of **1**−**8** at the MP2(full)/6-31+G* level of theory along with their protonated species, complexation with BH_3, and AuCl (B3LYP/6-31+G* plus def2-TZVPP), and coordinates for rotational transition states of **1**−**8**. This material is available free of charge via the Internet at http://pubs.acs.org.

AUTHOR INFORMATION

Corresponding Author

*E-mail: pvbharatam@niper.ac.in.

ACKNOWLEDGMENT

The authors thank the Department of Science and Technology (DST), New Delhi, for financial support. The authors also thank Prof. Gernot Frenking (University of Marburg, Germany) for useful suggestions. The authors thank the reviewers for useful suggestions.

REFERENCES

(1) (a) *Modern Allene Chemistry*; Krause, N., Hashmi, A. S. K., Eds.; Wiley-VCH, Verlag GmbH & Co. KGaA: Chichester, UK, 2008. (b) Taylor, D. R. *Chem. Rev.* **1967**, *67*, 317−359 and references cited therein.

(2) (a) Seeger, R.; Krishnan, R.; Pople, J. A.; Schleyer, P. v. R. *J. Am. Chem. Soc.* **1977**, *99*, 7103–7105. (b) Roth, W. R.; Ruf, G.; Ford, P. W. *Chem. Ber* **1974**, *107*, 48. (c) The rotational barrier of 1,2-d_2-ethylene (E = 65.0 kcal/mol measured by: Douglas, J. E.; Rabinowitch, B. S.; Looney, F. S. *J. Chem. Phys.* **1955**, *23*, 315–323) is reduced to 62.2 kcal/mol in *trans*-2-butene by alkyl substitution (Cundall, R. B.; Palmer, T. F. *Trans. Faraday Soc.* **1961**, *57*, 1936). On this basis, a barrier of −50 kcal/mol can be estimated for allene. (d) Furet, P.; Matcha, R. L.; Fuchs, R. *J. Phys. Chem.* **1986**, *90*, 5571–5573. (e) Bettinger, H. F.; Schreiner, P. R.; Schleyer, P. v. R.; Schaefer, H. F., III. *J. Phys. Chem.* **1996**, *100*, 16147–16154. (f) Kakkar, R. *Int. J. Quantum Chem.* **2004**, *94*, 93–104. (g) Cremeens, M. E.; Carpenter, B. K. *Org. Lett.* **2004**, *6*, 2349–2352. (h) Palmer, M. H. *Chem. Phys.* **2006**, *326*, 631–640. (i) Le, T. N.; Lee, H.-Y.; Mebel, A. M.; Kaiser, R. I. *J. Phys. Chem. A* **2001**, *105*, 1847–1856. (j) Dixon, D. A.; Smart, B. E. *J. Phys. Chem. A* **1989**, *93*, 7772–7780. (k) Novak, I. *J. Org. Chem.* **2001**, *66*, 3600–3601. (l) Rzepa, H. S. *Chem. Rev.* **2005**, *105*, 3697–3715. (m) Shakespeare, W. C.; Johnson, R. P. *J. Org. Chem.* **1991**, *56*, 6377–6379.

(3) (a) Kim, H.; Williams, L. J. *Curr. Opin. Drug Discovery Dev.* **2008**, *11*, 870–894. (b) Ma, S. *Chem. Rev.* **2005**, *105*, 2829–2872.

(4) (a) Ma, S. *Acc. Chem. Res.* **2009**, *42*, 1679–1688. (b) Samdja, W. *Chem. Rev.* **1983**, *83*, 263–320.

(5) Hoffmann-Röder, A.; Krause, N. *Angew. Chem., Int. Ed.* **2004**, *43*, 1196–1216.

(6) (a) Janssens, S.; Boon, G.; Geerlings, P. *J. Phys. Chem. A* **2006**, *110*, 9267–9272. (b) Weiss, R.; Wolf, H.; Schubert, U.; Clark, T. *J. Am. Chem. Soc.* **1981**, *103*, 6142–6147. (c) Dykstra, C. E. J. *J. Am. Chem. Soc.* **1977**, *99*, 2060–2063. (d) Honjou, N.; Pacansky, J.; Yoshimine, M. *J. Am. Chem. Soc.* **1984**, *106*, 5361–5364.

(7) (a) Jean, E.; Henri, R.; Leslie, R. *Organometallics* **2007**, *26*, 1542–1559. (b) Jean, E.; Henri, R.; Leslie, R. *Chem. Rev.* **2000**, *100*, 3639–3696. (c) Tidwell, T. T. *Acc. Chem. Res.* **1990**, *23*, 273–279. (d) Krow, G. R. *Angew. Chem., Int. Ed.* **1971**, *10*, 435–449. (e) Bock, H.; Solouki, B.; Bert, G.; Rosmus, P. *J. Am. Chem. Soc.* **1977**, *99*, 1663–1664. (f) Appel, R.; Fölling, P.; Josten, B.; Siray, M.; Winkhaus, V.; Knoch, F. *Angew. Chem., Int. Ed.* **1984**, *23*, 619–620. (g) Ozaki, S. *Chem. Rev.* **1972**, *72*, 457–496. (h) Williams, A.; Ibrahim, I. T. *Chem. Rev.* **1981**, *81*, 589–636. (i) Karsch, H. H.; Reisacher, H.-U.; Müller, G. *Angew. Chem., Int. Ed.* **1984**, *23*, 618–619.

(8) (a) Price, J. D.; Johnson, R. P. *Tetrahedron Lett.* **1986**, *27*, 4679–4682. (b) Hofmann, M. A.; Bergstrasser, T.; Reiss, G. J.; Nyulaszi, L.; Regitz, M. *Angew. Chem., Int. Ed.* **2000**, *39*, 1261–1263. (c) Shimizu, T.; Hojo, F.; Ando, W. *J. Am. Chem. Soc.* **1993**, *115*, 3111–3115. (d) Pang, Y.; Petrich, S. A.; Young, V. G.; Gordon, M. S.; Barton, T. J. *J. Am. Chem. Soc.* **1993**, *115*, 2534–2536.

(9) (a) Fernández, I.; Dyker, C. A.; DeHope, A.; Donnadieu, B.; Frenking, G.; Bertrand, G. *J. Am. Chem. Soc.* **2009**, *131*, 11875–11881. (b) Dyker, C. A.; Lavallo, V.; Donnadieu, B.; Bertrand, G. *Angew. Chem., Int. Ed.* **2008**, *47*, 3206–3209. (c) Hänninen, M. M.; Peuronen, A.; Tuononen., H. M. *Chem.—Eur. J.* **2009**, *15*, 7287–7291. (d) Johnson, R. P. *Chem. Rev.* **1989**, *89*, 1111–1124.

(10) Lavallo, V.; Dyker, C. A.; Donnadieu, B.; Bertrand, G. *Angew. Chem., Int. Ed.* **2008**, *47*, 5411–5414.

(11) Christl, M.; Engels, B. *Angew. Chem., Int. Ed.* **2009**, *48*, 1538–1539.

(12) Lavallo, V.; Dyker, C. A.; Donnadieu, B.; Bertrand, G. *Angew. Chem., Int. Ed.* **2009**, *48*, 1540–1542.

(13) (a) Kaufhold, O.; Hahn, F. E. *Angew. Chem., Int. Ed.* **2008**, *47*, 4057–4061. (b) Tonner, R.; Öxler, F.; Neumüller, B.; Petz, W.; Frenking, G. *Angew. Chem., Int. Ed.* **2006**, *45*, 8038–8042. (c) Tonner, R.; Frenking, G. *Angew. Chem., Int. Ed.* **2007**, *46*, 8695–8898. (d) Tonner, R.; Frenking, G . *Chem.—Eur. J.* **2008**, *14*, 3260–3272. (e) Tonner, R.; Frenking, G. *Chem.—Eur. J.* **2008**, *14*, 3273–3289. (f) Deshmukh, M. M.; Gadre, S. R.; Tonner, R.; Frenking, G. *Phys. Chem. Chem. Phys.* **2008**, *10*, 2298–2301. (g) Takagi, N.; Shimizu, T.; Frenking, G. *Chem.—Eur. J.* **2009**, *15*, 8593–8604. (h) Dyker, C. A.; Bertrand, G. *Nat. Chem.* **2009**, *1*, 265–266. (i) Frenking, G.; Tonner, R. *Pure Appl. Chem.* **2009**, *81*, 597–614. (j) Jablonski, M.; Palusiak, M. *Phys. Chem. Chem. Phys.* **2009**, *11*, 5711–5719. (k) Fürstner, A.; Alcarazo, M.; Goddard, R.; Lehmann, C. W. *Angew. Chem., Int. Ed.* **2008**, *47*, 3210–3214. (l) Alcarazo, M.; Lehmann, C. W.; Anoop, A.; Thiel, W.; Fürstner, A. *Nat. Chem.* **2009**, *1*, 295–301. (m) Takagi, N.; Shimizu, T.; Frenking, G. *Chem.—Eur. J.* **2009**, *15*, 3448–3457. (n) Patel, D. S.; Bharatam, P. V. *Curr. Sci.* **2010**, *99*, 425–426.

(14) (a) Viehe, H. G.; Janousek, Z.; Gompper, R.; Lach, D. *Angew. Chem., Int. Ed.* **1973**, *12*, 566–567. (b) Oeser, E. *Chem. Ber* **1974**, *107*, 627–633. (c) Janousek, Z.; Viehe, H. G. *Angew. Chem., Int. Ed.* **1971**, *10*, 574–575. (d) Taylor, M. J.; Surman, P. W. J.; Clark, G . R. *J. Chem. Soc., Chem. Commun.* **1994**, 2517–2518.

(15) Patel, D. S.; Bharatam, P. V. *Chem. Commun.* **2009**, 1064–1066.

(16) (a) Hariharan, M.; Rajan, S. S.; Srinivasan, R. *Acta Crystallogr.* **1989**, *C45*, 911–913. (b) Bharatam, P. V.; Patel, D. S.; Iqbal, P. *J. Med. Chem.* **2005**, *48*, 7615–7622. (c) Sundriyal, S.; Khanna, S.; Saha, R.; Bharatam, P. V. *J. Phys. Org. Chem.* **2008**, *21*, 30–33.

(17) (a) Hehre, W. J.; Radom, L.; Schleyer, P. v. R.; Pople, J. A. *Ab Initio Molecular Orbital Theory*; Wiley: New York, 1985. (b) Foresman, J. B.; Frisch, Æ. *Exploring Chemistry with Electronic Structure Methods*; Gaussian Inc.: Pittsburgh, PA, 1998. (c) Ochterski, J. W. *Thermochemistry in Gaussian*. http://Gaussian.com/g_whitepap/thermo.htm.

(18) (a) Parr, R. G.; Yang, W.*Density Functional Theory of Atoms and Molecules*; Oxford University Press: New York, 1989. (b) Bartolotti, L. J.; Fluchick, K. In *Reviews in Computational Chemistry*; Lipkowitz, K. B., Boyd, D. B., Eds.; VCH Publishers: New York, 1996; Vol. 7, p 187.

(19) (a) Frisch, M. J.; Trucks, G. W.; Schlegel, H. B.; Scuseria, G. E.; Robb, M. A.; Cheeseman, J. R.; Montgomery, J. A., Jr.; Vreven, T.; Kudin, K. N.; Burant, J. C.; Millam, J. M.; Iyengar, S. S.; Tomasi, J.; Barone, V.; Mennucci, B.; Cossi, M.; Scalmani, G.; Rega, N.; Petersson, G. A.; Nakatsuji, H.; Hada, M.; Ehara, M.; Toyota, K.; Fukuda, R.; Hasegawa, J.; Ishida, M.; Nakajima, T.; Honda, Y.; Kitao, O.; Nakai, H.; Klene, M.; Li, X.; Knox, J. E.; Hratchian, H. P.; Cross, J. B.; Adamo, C.; Jaramillo, J.; Gomperts, R.; Stratmann, R. E.; Yazyev, O.; Austin, A. J.; Cammi, R.; Pomelli, C.; Ochterski, J. W.; Ayala, P. Y.; Morokuma, K.; Voth, G. A.; Salvador, P.; Dannenberg, J. J.; Zakrzewski, V. G.; Dapprich, S.; Daniels, A. D.; Strain, M. C.; Farkas, O.; Malick, D. K.; Rabuck, A. D.; Raghavachari, K.; Foresman, J. B.; Ortiz, J. V.; Cui, Q.; Baboul, A. G.; Clifford, S.; Cioslowski, J.; Stefanov, B. B.; Liu, G.; Liashenko, A.; Piskorz, P.; Komaromi, I.; Martin, R. L.; Fox, D. J.; Keith, T.; Al-Laham, M. A.; Peng, C. Y.; Nanayakkara, A.; Challacombe, M.; Gill, P. M. W.; Johnson, B.; Chen, W.; Wong, M. W.; Gonzalez, C.; Pople, J. A. *Gaussian 03*, Revision C.02, Gaussian, Inc., Wallingford, CT, 2004. (b) See the Supporting Information.

(20) (a) Becke, A. D. *J. Chem. Phys.* **1993**, *98*, 5648–5652. (b) Lee, C.; Yang, W.; Parr, R. G. *Phys. Rev. B* **1988**, *37*, 785–789. (c) Perdew, J. P.; Wang, Y. *Phys. Rev. B* **1992**, *45*, 13244–13249.

(21) Krishan, R.; Frisch, M. J.; Pople, J. A. *J. Chem. Phys.* **1980**, *72*, 4244–4245.

(22) Scott, A. P.; Radom, L. *J. Phys. Chem.* **1996**, *100*, 16502–16513.

(23) Curtiss, L. A.; Raghavachari, K.; Pople, J. A. *J. Chem. Phys.* **1993**, *98*, 1293–1298.

(24) (a) Reed, A. E.; Weinstock, R. B.; Wienhold, F. *J. Chem. Phys.* **1985**, *83*, 735–746. (b) Reed, A. E.; Curtiss, L. A.; Wienhold, F. *Chem. Rev.* **1988**, *88*, 899–926.

(25) Weigend, F.; Ahlrichs, R. *Phys. Chem. Chem. Phys.* **2005**, *7*, 3297–3305.

(26) Jarowski, P. D.; Diederich, F.; Houk, K. N. *J. Phys. Chem. A* **2006**, *110*, 7237–7246.

(27) Lam, B.; Johnson, R. P. *J. Am. Chem. Soc.* **1983**, *105*, 7439–7483.

(28) Pinkerton, A. A.; Schwarzenbach, D. *J. Chem. Soc., Dalton Trans.* **1978**, 989–996.

(29) Apeloig and co-workers showed that BH_2 substitution in $R_2Si{=}Si{=}SiR_2$ imposes linear character across Si═Si═Si. Following this, $(H_2B)_2C{=}C{=}C(BH_2)_2$ has been found to be clearly linear at the B3LYP/6-31+G* level of theory.